



Supplement of

Exploring the chemical fate of the sulfate radical anion by reaction with sulfur dioxide in the gas phase

N. T. Tsone et al.

Correspondence to: N. T. Tsone (narcisse.tsonatchinda@helsinki.fi)

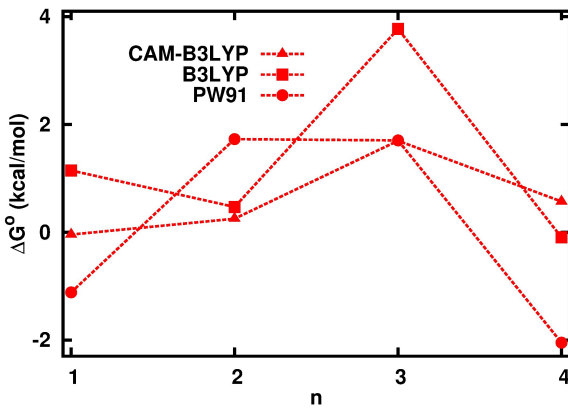


Figure S1: Gibbs free energies of hydration (in kcal mol^{-1}) of the $\text{SO}_3\text{SO}_3^-(\text{H}_2\text{O})_{n-1}$ anion from DFT using the aug-cc-pVDZ basis set, calculated at 1 atm and 298.15 K . Different functionals are used for comparison. Color coding is similar to Fig. 4 in the main article.

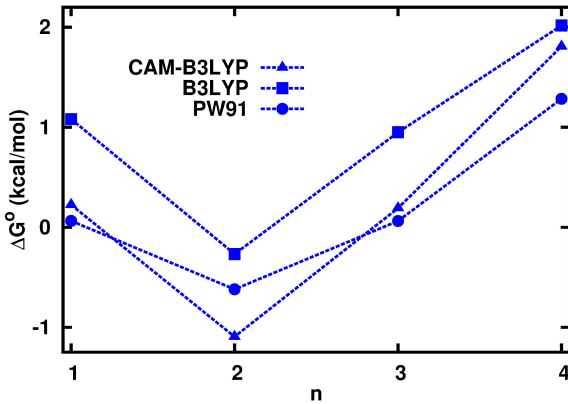


Figure S2: Gibbs free energies of hydration (in kcal mol^{-1}) of the $\text{SO}_2\text{SO}_4^-(\text{H}_2\text{O})_{n-1}$ anion from DFT using the aug-cc-pVDZ basis set, calculated at 1 atm and 298.15 K . Different functionals are used for comparison. Color coding is similar to Fig. 4 in the main article.

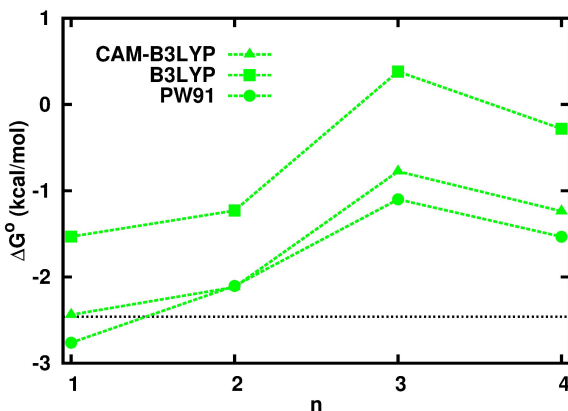


Figure S3: Gibbs free energies of hydration (in kcal mol^{-1}) of the $\text{SO}_4^-(\text{H}_2\text{O})_{n-1}$ anion from DFT using the aug-cc-pVDZ basis set, calculated at 1 atm and 298.15 K . Different functionals are used for comparison. The black dotted line delimits the domains where water condensation is favoured (below the dotted line) and where water evaporation is favoured (above the dotted line). Color coding is similar to Fig. 4 in the main article.

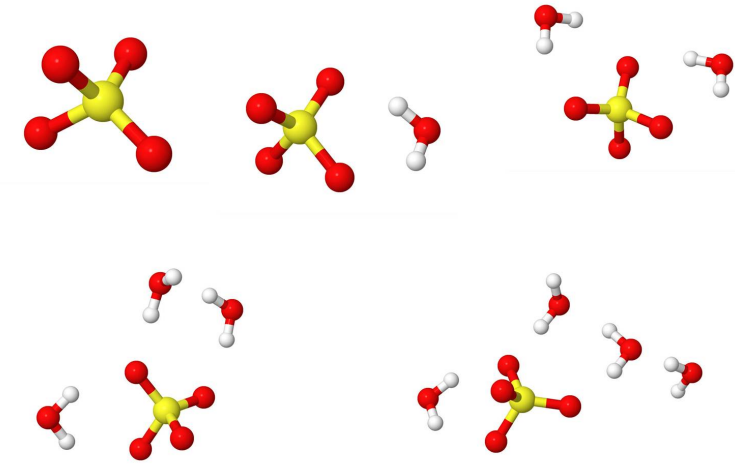


Figure S4: Ground state structures $\text{SO}_4^- (\text{H}_2\text{O})_{0-4}$, and b) $\text{SO}_3\text{SO}_3^- (\text{H}_2\text{O})_{3-4}$, calculated using the CAM-B3LYP/aug-cc-pVDZ method. Colour coding: yellow = sulphur, red = oxygen, and white = hydrogen

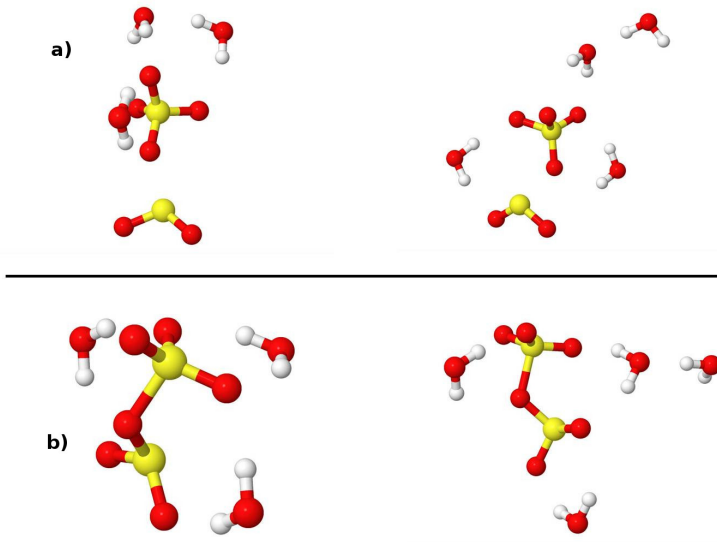


Figure S5: Ground state structures of a) $\text{SO}_2\text{SO}_4^- (\text{H}_2\text{O})_{3-4}$, and b) $\text{SO}_3\text{SO}_3^- (\text{H}_2\text{O})_{3-4}$, calculated using the CAM-B3LYP/aug-cc-pVDZ method. Colour coding: yellow = sulphur, red = oxygen, and white = hydrogen

Table S1: Gibbs free energy (ΔG° at 298.15 K) and enthalpy (ΔH°) of the most stable species involved in the SO_2 and $\text{SO}_4^- (\text{H}_2\text{O})_n$ collisions, calculated at the CCSD(T)/aug-cc-pVDZ//CAM-B3LYP/aug-cc-pVDZ level of theory. The ΔG° 's are shown in Fig. 3 in the main article. The energies are calculated relative to $\text{SO}_2 + \text{SO}_4^- (\text{H}_2\text{O})_n$ and the units are kcal mol⁻¹.

n	$\text{SO}_2\text{SO}_4^- (\text{H}_2\text{O})_n$		Transition state		$\text{SO}_3\text{SO}_3^- (\text{H}_2\text{O})_n$		$\text{SO}_3 + \text{SO}_3^- (\text{H}_2\text{O})_n$	
	ΔG°	ΔH°	ΔG°	ΔH°	ΔG°	ΔH°	ΔG°	ΔH°
0	-5.6	-14.1	4.4	-5.6	-9.5	-19.4	11.9	11.7
1	-3.6	-11.7	5.2	-5.4	-7.3	-18.0	10.4	10.0
2	-2.5	-10.3	8.3	-3.8	-5.1	-15.0	9.8	9.4

Table S2: Gibbs free energy (ΔG° at 298.15 K) and enthalpy (ΔH°) of hydration of the $\text{SO}_4^- (\text{H}_2\text{O})_{n-1}$, $\text{SO}_2\text{SO}_4^- (\text{H}_2\text{O})_{n-1}$, and $\text{SO}_3\text{SO}_3^- (\text{H}_2\text{O})_{n-1}$ anions, calculated at the CCSD(T)/aug-cc-pVDZ//CAM-B3LYP/aug-cc-pVDZ level of theory. The ΔG° 's are shown in Fig. 4 in the main article. Units are kcal mol⁻¹.

n	$\text{SO}_4^- (\text{H}_2\text{O})_{n-1}$		$\text{SO}_2\text{SO}_4^- (\text{H}_2\text{O})_{n-1}$		$\text{SO}_3\text{SO}_3^- (\text{H}_2\text{O})_{n-1}$	
	ΔG°	ΔH°	ΔG°	ΔH°	ΔG°	ΔH°
0	-3.3	-11.9	-1.3	-6.7	-1.0	-8.5
1	-3.1	-11.3	-1.9	-7.2	-0.9	-6.2

Table S3: Gibbs free energies (in kcal mol⁻¹) of hydration of the $\text{SO}_4^- (\text{H}_2\text{O})_{n-1}$, $\text{SO}_2\text{SO}_4^- (\text{H}_2\text{O})_{n-1}$ and $\text{SO}_3\text{SO}_3^- (\text{H}_2\text{O})_{n-1}$ anions, calculated using three different functionals and the aug-cc-pVDZ basis set.

n	$\text{SO}_4^- (\text{H}_2\text{O})_{n-1}$			$\text{SO}_2\text{SO}_4^- (\text{H}_2\text{O})_{n-1}$			$\text{SO}_3\text{SO}_3^- (\text{H}_2\text{O})_{n-1}$		
	B3LYP	CAM-B3LYP	PW91	B3LYP	CAM-B3LYP	PW91	B3LYP	CAM-B3LYP	PW91
1	-1.5	-2.4	-2.8	1.1	0.2	0.1	1.1	-0.1	-1.1
2	-1.2	-2.1	-2.1	-0.3	-1.1	-0.6	0.5	0.3	1.7
3	0.4	-0.8	-1.1	0.9	0.2	0.1	3.8	1.7	1.7
4	-0.3	-1.2	-1.5	2.0	0.9	1.3	-0.1	0.6	-2.0

Table S4: Collision rate constant ($k_{\text{coll},(\text{R1})}$) of SO_2 and $\text{SO}_4^- (\text{H}_2\text{O})_n$, oxidation rate constant ($k_{\text{ox},(\text{R2a})}$) of SO_2 in the $\text{SO}_2\text{SO}_4^- (\text{H}_2\text{O})_n$ reactant complex, and evaporation rate constant ($k_{\text{evap},(\text{R2b})}$) of SO_2 from $\text{SO}_2\text{SO}_4^- (\text{H}_2\text{O})_n$, for Reactions (R1), (R2a), and (R2b), respectively in the main article. Calculations are performed at 298 K.

n	$k_{\text{coll},(\text{R1})}$ (cm ³ s ⁻¹)	$k_{\text{ox},(\text{R2a})}$ (s ⁻¹)	$k_{\text{evap},(\text{R2b})}$ (s ⁻¹)
0	1.4×10^{-9}	$2.8 \times 10^{+5}$	$2.3 \times 10^{+6}$
1	1.4×10^{-9}	$2.2 \times 10^{+6}$	$6.1 \times 10^{+7}$
2	1.3×10^{-9}	$7.7 \times 10^{+4}$	$4.1 \times 10^{+8}$

Table S5: Relative concentration of the most stable anionic species involved in the $\text{SO}_2 + \text{SO}_4^- (\text{H}_2\text{O})_n \rightarrow \text{SO}_3\text{SO}_3^- (\text{H}_2\text{O})_n$ reaction at thermal equilibrium, calculated with a) actual values of the Gibbs free energies of formation, b) with -1 kcal mol⁻¹ uncertainty and c) +1 kcal mol⁻¹ uncertainty on the Gibbs free energy of formation. These are calculated at different SO_2 concentrations, different relative humidities, and $T = 298.15$ K. See also Figs. 5, S6 and S7.

Species	RH = 10 %			RH = 50 %			RH = 90 %		
	2 ppb SO_2	200 ppb SO_2	a)	2 ppb SO_2	200 ppb SO_2	2 ppb SO_2	200 ppb SO_2	2 ppb SO_2	200 ppb SO_2
SO_4^-	45.3	24.9		6.5	5.7	2.4	2.2		
$\text{SO}_4^- (\text{H}_2\text{O})_1$	35.5	18.9		24.6	21.8	16.1	15.4		
$\text{SO}_4^- (\text{H}_2\text{O})_2$	19.3	10.6		68.9	61.1	81.5	77.6		
SO_2SO_4^-	1.1×10^{-3}	6.2×10^{-2}		1.6×10^{-4}	1.4×10^{-2}	5.8×10^{-5}	5.6×10^{-3}		
$\text{SO}_2\text{SO}_4^- (\text{H}_2\text{O})_1$	3.2×10^{-5}	1.8×10^{-3}		2.3×10^{-5}	2.0×10^{-3}	1.5×10^{-5}	1.4×10^{-3}		
$\text{SO}_2\text{SO}_4^- (\text{H}_2\text{O})_2$	2.6×10^{-6}	1.4×10^{-4}		9.3×10^{-6}	8.3×10^{-4}	1.1×10^{-5}	1.0×10^{-3}		
SO_3SO_3^-	0.8	44.7		0.1	10.3	4.2×10^{-2}	4.0		
$\text{SO}_3\text{SO}_3^- (\text{H}_2\text{O})_1$	1.5×10^{-2}	0.8		1.1×10^{-2}	0.9	7.0×10^{-3}	0.7		
$\text{SO}_3\text{SO}_3^- (\text{H}_2\text{O})_2$	2.3×10^{-4}	1.3×10^{-2}		8.1×10^{-4}	0.1	9.6×10^{-4}	0.1		
			b)						
SO_4^-	5.5	82.2		0.3	47.0	0.1	28.6		
$\text{SO}_4^- (\text{H}_2\text{O})_1$	22.7	11.5		6.2	33.0	3.5	36.1		
$\text{SO}_4^- (\text{H}_2\text{O})_2$	68.7	1.2		93.3	17.1	96.3	33.6		
SO_2SO_4^-	7.4×10^{-4}	3.7×10^{-2}		4.0×10^{-5}	2.1×10^{-2}	1.3×10^{-5}	1.3×10^{-2}		
$\text{SO}_2\text{SO}_4^- (\text{H}_2\text{O})_1$	1.1×10^{-4}	2.0×10^{-4}		3.1×10^{-5}	5.6×10^{-4}	1.7×10^{-5}	6.1×10^{-4}		
$\text{SO}_2\text{SO}_4^- (\text{H}_2\text{O})_2$	5.0×10^{-5}	3.0×10^{-6}		6.8×10^{-5}	4.2×10^{-5}	7.0×10^{-5}	8.3×10^{-5}		
SO_3SO_3^-	2.9	5.0		0.2	2.8	4.9×10^{-2}	1.7		
$\text{SO}_3\text{SO}_3^- (\text{H}_2\text{O})_1$	2.8×10^{-1}	1.7×10^{-2}		7.7×10^{-2}	4.8×10^{-2}	4.4×10^{-2}	5.3×10^{-2}		
$\text{SO}_3\text{SO}_3^- (\text{H}_2\text{O})_2$	2.3×10^{-2}	4.8×10^{-5}		3.2×10^{-2}	6.8×10^{-4}	3.3×10^{-2}	1.3×10^{-3}		
			c)						
SO_4^-	86.5	1.3		48.4	0.2	29.1	8.5×10^{-2}		
$\text{SO}_4^- (\text{H}_2\text{O})_1$	12.1	5.5		34.0	4.9	36.7	3.1		
$\text{SO}_4^- (\text{H}_2\text{O})_2$	1.3	16.6		17.6	73.9	34.2	85.5		
SO_2SO_4^-	3.9×10^{-4}	1.8×10^{-2}		2.2×10^{-4}	3.2×10^{-3}	1.3×10^{-4}	1.1×10^{-3}		
$\text{SO}_2\text{SO}_4^- (\text{H}_2\text{O})_1$	2.1×10^{-6}	2.7×10^{-3}		5.8×10^{-6}	2.4×10^{-3}	6.2×10^{-6}	1.6×10^{-3}		
$\text{SO}_2\text{SO}_4^- (\text{H}_2\text{O})_2$	3.1×10^{-8}	1.2×10^{-3}		4.4×10^{-7}	5.4×10^{-3}	8.5×10^{-7}	6.2×10^{-3}		
SO_3SO_3^-	5.2×10^{-2}	69.1		3.0×10^{-2}	12.3	1.8×10^{-2}	4.4		
$\text{SO}_3\text{SO}_3^- (\text{H}_2\text{O})_1$	1.7×10^{-4}	6.9		5.0×10^{-4}	6.1	5.4×10^{-4}	3.9		
$\text{SO}_3\text{SO}_3^- (\text{H}_2\text{O})_2$	5.0×10^{-7}	0.6		7.0×10^{-6}	2.5	1.4×10^{-5}	2.9		

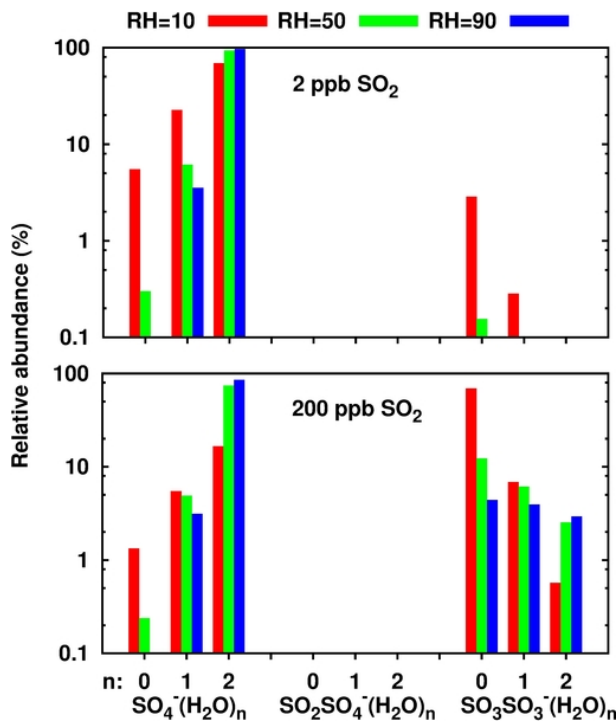


Figure S6: Distribution of the most stable anions in the reaction between SO_2 and $\text{SO}_4^-(\text{H}_2\text{O})_n$ at thermal equilibrium, assuming general underbinding of the CAM-B3LYP/CCSD(T) method of 1 kcal mol⁻¹ in Gibbs free energy of hydration. Concentrations are calculated for 2 ppb and 200 ppb of SO_2 and relative humidity RH = 10, 50, and 90 %. The temperature is 298.15 K. Data are shown in Table S5b.

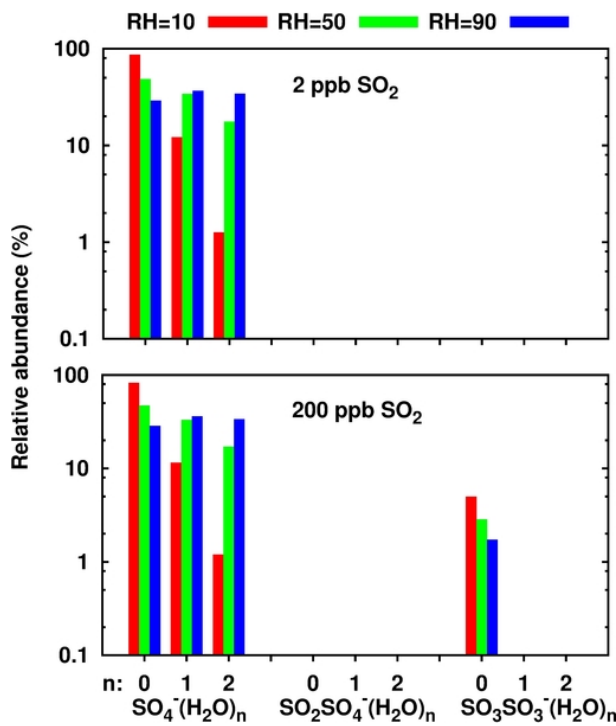


Figure S7: Distribution of the most stable anions in the reaction between SO_2 and $\text{SO}_4^-(\text{H}_2\text{O})_n$ at thermal equilibrium, assuming general overbinding of the CAM-B3LYP/CCSD(T) method of 1 kcal mol⁻¹ in Gibbs free energy of hydration. Concentrations are calculated for 2 ppb and 200 ppb of SO_2 and relative humidity RH = 10, 50, and 90 %. The temperature is 298.15 K. Data are shown in Table S5c.

Table S6: Harmonic frequencies (in cm^{-1}) of the most stable $\text{SO}_2\text{SO}_4^-(\text{H}_2\text{O})_n$, transition state, and $\text{SO}_3\text{SO}_3^-(\text{H}_2\text{O})_n$ structures shown in Fig. 2 in the main article.

$\text{SO}_2\text{SO}_4^-(\text{H}_2\text{O})_n$			Transition state			$\text{SO}_3\text{SO}_3^-(\text{H}_2\text{O})_n$		
$n = 0$	$n = 1$	$n = 2$	$n = 0$	$n = 1$	$n = 2$	$n = 0$	$n = 1$	$n = 2$
21	19	17	i497	i427	i485	15	18	12
28	26	21	27	22	27	19	24	19
61	38	27	42	30	31	120	38	22
107	43	36	94	55	41	252	104	33
136	81	39	159	81	49	268	114	48
270	86	54	180	100	77	338	152	82
332	102	73	320	155	83	405	255	124
371	158	87	347	192	96	457	271	142
373	213	106	461	222	170	498	335	144
503	288	140	498	296	181	506	372	265
518	328	155	504	314	196	538	400	269
538	334	224	523	345	217	594	410	270
689	348	263	626	364	320	784	462	277
913	421	272	944	489	347	1004	498	303
1092	508	281	1106	493	356	1041	507	313
1140	521	299	1149	526	377	1158	537	357
1213	527	337	1233	538	388	1255	562	407
1261	615	357	1247	610	447	1272	597	462
	683	397		643	488		785	498
	912	507		982	495		1005	520
	1132	519		1110	517		1039	537
	1148	537		1178	531		1158	550
	1209	562		1229	660		1247	576
	1277	577		1253	716		1282	629
	1684	694		1684	751		1679	748
	3766	919		3757	968		3755	1000
	3807	1127		3812	1111		3825	1046
		1147			1151			1174
		1180			1233			1238
		1280			1253			1245
		1666			1669			1668
		1679			1686			1680
		3749			3597			3784
		3771			3646			3786
		3848			3837			3839
		3864			3857			3842

Table S7: CAM-B3LYP/aug-cc-pVDZ Cartesian coordinates (in angström) of the most stable reactant complexes shown in Fig. 2a in the main article.

SO_2SO_4^-			
O	2.825107	0.156760	-1.355518
O	2.363947	1.064713	0.947284
S	2.209459	-0.138952	-0.012337
O	2.666257	-1.420147	0.562402
O	0.670207	0.008367	-0.061607
S	2.127117	2.248396	-2.372085
O	3.445617	2.908847	-2.503388
O	1.576002	1.727531	-3.643685
$\text{SO}_2\text{SO}_4^-(\text{H}_2\text{O})_1$			
S	1.980451	0.641827	0.721950
O	1.139850	-0.591538	0.328050
O	2.783577	0.590480	-0.623185
O	2.855993	0.400330	1.894622
O	1.160261	1.880159	0.806900
O	2.321708	2.940800	3.312736
H	1.735131	2.957448	2.541186
H	2.745530	2.078596	3.184058
S	-0.787099	0.125042	-1.313735
O	-0.609772	-0.866320	-2.395438
O	-1.964964	-0.101901	-0.452406
$\text{SO}_2\text{SO}_4^-(\text{H}_2\text{O})_2$			
S	1.439944	0.973647	1.793171
O	0.631056	-0.213030	1.371916
O	2.630048	1.218150	0.831591
O	1.856718	0.909621	3.220749
O	0.766009	2.306109	1.423134
O	1.867679	3.763925	3.954101
H	2.004482	2.803407	3.982481
H	1.444814	3.869923	3.092787
S	-0.058883	-0.142039	-1.127406
O	0.547748	-1.404722	-1.595099
O	-1.529623	-0.166151	-0.995913
O	0.782775	-1.732526	4.006224
H	1.235760	-0.878163	4.074384
H	0.471752	-1.702303	3.091549

Table S8: CAM-B3LYP/aug-cc-pVDZ Cartesian coordinates (in Angström) of transition states of Reaction (R2a) shown in Fig. 2b in the main article.

Unhydrated transition state			
S	-1.446236	0.004819	-0.101278
O	-2.266101	-0.061322	1.170106
O	-1.687144	1.206203	-0.931491
O	-1.328814	-1.269272	-0.844527
O	-0.050817	0.239308	0.745785
S	1.759857	0.046819	-0.225163
O	2.550753	1.150015	0.370711
O	2.255850	-1.316524	0.065664
Monohydrated transition state			
O	-2.329767	-0.421493	0.517842
S	-1.196992	-0.239488	-0.441137
O	-0.006242	-0.051023	0.748501
S	1.855338	0.424969	-0.004021
O	2.791611	-0.563594	0.572228
O	-1.189201	1.013112	-1.225791
O	-0.815365	-1.459901	-1.201766
O	2.116984	1.844369	0.311342
O	-2.629181	-3.364716	0.112114
H	-1.924277	-3.068719	-0.485471
H	-2.847237	-2.526576	0.545472
Dihydrated transition state			
O	-2.567018	-0.272583	0.270936
S	-1.419593	-0.021122	-0.667424
O	-0.335635	0.246156	0.546368
S	1.668734	0.141362	0.066934
O	2.123141	-1.204656	0.475244
O	-1.500465	1.206192	-1.480792
O	-0.945216	-1.229555	-1.401743
O	2.276825	1.281250	0.784734
O	0.701323	-3.788804	1.694419
H	1.214615	-3.038128	1.371561
H	-0.180803	-3.656497	1.296207
O	-1.768424	-3.247548	0.390130
H	-1.422550	-2.748183	-0.374576
H	-2.284127	-2.564373	0.839504

Table S9: CAM-B3LYP/aug-cc-pVDZ Cartesian coordinates (in angström) of the most stable products shown in Fig. 2c in the main article.

SO_3SO_3^-			
O	-2.285527	-1.272200	0.074224
O	1.354358	-1.253234	-0.844887
S	-1.532961	0.004227	-0.134058
O	-2.281204	1.283057	0.075057
O	-0.217287	0.001692	0.802499
S	1.430941	-0.000759	-0.066685
O	1.358507	1.252459	-0.844088
O	2.275230	-0.002543	1.139135
$\text{SO}_3\text{SO}_3^-(\text{H}_2\text{O})_1$			
O	-2.063805	0.700313	-1.360015
S	-0.968260	1.022031	-0.420948
O	-0.058720	-0.560305	-0.525162
S	0.688809	-1.095623	0.814563
O	1.877765	-0.257936	1.145047
O	-1.308100	1.080047	1.014685
O	0.031778	1.992716	-0.911407
O	0.886521	-2.561979	0.605815
O	-1.101392	2.329077	-3.656536
H	-0.441615	2.483259	-2.964533
H	-1.689470	1.706418	-3.203686
$\text{SO}_3\text{SO}_3^-(\text{H}_2\text{O})_2$			
O	-1.667021	0.614603	-0.966407
S	-0.529326	1.317177	-0.335222
O	0.744377	0.055458	-0.294183
S	0.398848	-1.301994	0.561063
O	1.342783	-1.377415	1.713003
O	-0.693795	1.664172	1.092608
O	0.181790	2.307262	-1.176177
O	0.349590	-2.449484	-0.389988
O	-1.377994	1.775058	-3.714589
H	-0.676964	2.208156	-3.207836
H	-1.754491	1.186529	-3.044135
O	0.893961	4.209023	1.063875
H	0.393316	3.493059	1.481254
H	0.913757	3.909106	0.144287

Table S10: CAM-B3LYP/aug-cc-pVDZ Cartesian coordinates (in angström) of the most stable structures of the $\text{SO}_4^- (\text{H}_2\text{O})_{0-4}$ clusters shown in Fig. S4.

SO_4^-			
S	2.268180	-0.314113	0.205473
O	2.554359	-1.358683	1.224658
O	1.378257	-0.853588	-0.949971
O	3.473479	0.393977	-0.301899
O	1.164349	0.674077	0.675067
$\text{SO}_4^- (\text{H}_2\text{O})_1$			
S	1.906184	0.300765	0.629427
O	1.954000	-0.555414	1.931587
O	1.487465	-0.496567	-0.546337
O	3.173888	1.064491	0.431411
O	0.777454	1.199570	1.190354
O	2.695419	3.493176	1.874809
H	1.804740	3.136465	1.988185
H	3.108681	2.765902	1.373909
$\text{SO}_4^- (\text{H}_2\text{O})_2$			
S	1.749710	-0.344864	0.539446
O	1.325734	-1.189596	1.772307
O	1.453869	-1.036391	-0.741743
O	3.166951	0.120211	0.648409
O	0.746441	0.777904	0.870986
O	2.879211	2.568345	2.189644
H	1.936397	2.410732	2.051016
H	3.258574	1.796765	1.735107
O	4.098258	-0.938203	-1.980871
H	4.251247	-0.473168	-1.145409
H	3.153709	-1.141981	-1.887858
$\text{SO}_4^- (\text{H}_2\text{O})_3$			
S	1.258300	0.501845	0.344904
O	1.006506	-0.893458	0.977068
O	0.494646	0.700203	-0.907892
O	2.728304	0.771018	0.200623
O	0.668078	1.246315	1.554401
O	3.371549	1.843489	2.862725
H	2.409868	1.809424	2.948668
H	3.485590	1.499755	1.962075
O	4.107635	0.773258	-2.189359
H	3.610117	0.838893	-1.345411
H	4.320861	-0.162490	-2.258909
O	1.595725	1.053253	-3.639167
H	1.089974	0.957606	-2.816715
H	2.514009	1.037275	-3.321846
$\text{SO}_4^- (\text{H}_2\text{O})_4$			
S	1.294648	0.829604	0.754062
O	0.682168	-0.591592	0.850668
O	0.596819	1.678308	-0.241181
O	2.780360	0.766038	0.545357
O	0.946047	1.173487	2.209746
O	3.752560	0.531388	3.314925
H	2.825490	0.702100	3.524548
H	3.729850	0.548352	2.344760
O	4.009743	1.282920	-1.849133
H	3.595161	1.139198	-0.969385
H	4.076827	0.400502	-2.226829
O	1.664202	2.582293	-2.751495
H	1.179286	2.338610	-1.943770
H	2.554725	2.217780	-2.593234
O	1.437630	5.111557	-3.795125
H	1.504847	4.195849	-3.441397
H	1.655212	5.666914	-3.041057

Table S11: CAM-B3LYP/aug-cc-pVDZ Cartesian coordinates (in angström) of the most stable structures of the $\text{SO}_2\text{SO}_4^- (\text{H}_2\text{O})_{3-4}$ clusters shown in Fig. S5a.

$\text{SO}_2\text{SO}_4^- (\text{H}_2\text{O})_3$			
S	1.414410	0.693869	1.864708
O	0.518148	-0.389474	1.367880
O	2.664687	0.867637	0.975102
O	1.746282	0.561959	3.311554
O	0.884132	2.104560	1.516730
O	2.630729	3.219534	3.921180
H	2.409315	2.270545	3.941517
H	2.031952	3.551587	3.240355
S	-0.076135	-0.139273	-1.195446
O	0.359184	-1.459921	-1.690198
O	-1.537497	0.052196	-1.114913
O	0.200977	-1.885429	4.010308
H	0.785756	-1.121833	4.125521
H	-0.014068	-1.816470	3.070636
O	4.847620	2.809678	2.093716
H	4.238710	3.052357	2.812815
H	4.341987	2.149439	1.600806
$\text{SO}_2\text{SO}_4^- (\text{H}_2\text{O})_4$			
S	1.936171	0.245397	2.001379
O	1.051009	-0.849657	1.506501
O	3.311290	0.256103	1.300433
O	2.051453	0.274115	3.485247
O	1.544619	1.622665	1.416702
O	3.776505	-0.748951	-1.500937
H	3.720108	-0.387917	-0.604081
H	2.995277	-1.313153	-1.573054
S	0.177754	-0.823449	-0.934415
O	0.979594	-1.950046	-1.461051
O	-1.240975	-1.132978	-0.684607
O	0.201620	-1.911968	4.289763
H	0.843315	-1.187614	4.336517
H	0.084135	-2.004954	3.335910
O	2.369628	3.066408	4.031937
H	2.348188	2.094716	4.088871
H	2.149745	3.222742	3.105091
O	0.992378	4.606902	5.900022
H	0.170481	4.121763	6.018151
H	1.498765	4.070181	5.255958

Table S12: CAM-B3LYP/aug-cc-pVDZ Cartesian coordinates (in angström) of the most stable structures of the $\text{SO}_3\text{SO}_3^-(\text{H}_2\text{O})_{3-4}$ clusters shown in Fig. S5b.

$\text{SO}_3\text{SO}_3^-(\text{H}_2\text{O})_3$			
O	-0.002636	-1.685922	-2.075659
S	0.000070	-1.221334	-0.688881
O	-0.000171	0.573761	-1.008332
S	-0.001696	1.557847	0.270847
O	-1.281876	2.328444	0.275157
O	1.247158	-1.390544	0.096699
O	-1.243694	-1.390334	0.101841
O	1.274561	2.334934	0.272220
O	-3.646486	0.368520	-0.072727
H	-3.014706	-0.364722	-0.108163
H	-3.074826	1.142026	0.021569
O	3.643893	0.378200	-0.078954
H	3.014328	-0.356945	-0.114000
H	3.070293	1.150342	0.014537
O	0.011539	-1.929643	2.799764
H	-0.743149	-1.828683	2.203588
H	0.755790	-1.825558	2.190939
$\text{SO}_3\text{SO}_3^-(\text{H}_2\text{O})_4$			
O	-1.701694	-0.177303	0.733943
S	-1.217066	-0.438033	-0.633029
O	0.381928	-1.342003	-0.246816
S	1.774685	-0.564055	-0.420968
O	2.843843	-1.609578	-0.441792
O	-0.709184	0.735106	-1.383087
O	-1.879186	-1.489690	-1.406798
O	1.925341	0.543144	0.577574
O	4.872580	-0.377792	1.407958
H	4.190638	0.286837	1.563522
H	4.444492	-0.975569	0.778598
O	-1.353742	-2.356753	2.654338
H	-0.528812	-2.681485	2.278889
H	-1.587328	-1.611639	2.076685
O	0.419303	3.049629	-0.132190
H	-0.159210	2.400304	-0.566186
H	1.064946	2.486773	0.315582
O	1.344967	5.217555	-1.599711
H	1.004202	4.469603	-1.065358
H	1.729543	4.798410	-2.374890